

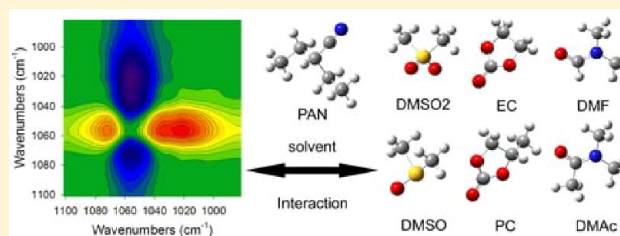
Interactions between Polyacrylonitrile and Solvents: Density Functional Theory Study and Two-Dimensional Infrared Correlation Analysis

Qing-Yun Wu,[†] Xiao-Na Chen,[†] Ling-Shu Wan, and Zhi-Kang Xu*

MOE Key Laboratory of Macromolecular Synthesis and Functionalization, Department of Polymer Science and Engineering, Zhejiang University, Hangzhou 310027, People's Republic of China

S Supporting Information

ABSTRACT: Polyacrylonitrile (PAN) is a semicrystalline polymer with high polarity and is usually processed from solutions. Selected solvents for processing influence both the structure and properties of PAN products. We describe the interactions between PAN and various solvents by theoretical calculation based on density functional theories (DFT), and by experimental methods of Fourier transform infrared (FTIR) spectra and two-dimensional infrared (2D-IR) correlation analysis. The selected solvents include dimethyl sulfone (DMSO₂), dimethyl sulfoxide (DMSO), ethylene carbonate (EC), propylene carbonate (PC), *N,N*-dimethyl formamide (DMF), and *N,N*-dimethyl acetamide (DMAc). Calculation results show that the PAN model monomer (PAN') interacts with each solvent through dipole–dipole interaction and formed PAN'–solvent complexes. Each complex displays an antiparallel alignment of interacting pair between the C≡N group of PAN' and the polar group of solvent molecule (S=O or C=O group). The calculated binding energies (ΔE) reveal that PAN' preferentially interacts with solvent in the order of DMSO₂ > DMSO > EC > PC > DMF > DMAc. Red shifts of vibration frequencies are observed for C≡N, S=O, and C=O stretching bands. The C≡N stretching band shifts from 2245 cm⁻¹ in PAN to 2240, 2242, and 2241 cm⁻¹ in PAN–DMSO, PAN–EC, and PAN–DMF mixtures, respectively, indicating the existence of PAN–solvent interactions. Moreover, 2D-IR correlation analysis shows that as the PAN content increases, DMSO molecules vary prior to PAN–DMSO complexes, and change earlier than PAN bulk. However, PAN–EC and PAN–DMF mixtures follow the order of PAN bulk > PAN–solvent complexes > solvent molecules. This combination of theoretical simulation and experimental characterization is useful in selection of solvents for PAN or even other polar polymers and can provide an insight into the physical behavior of PAN–solvent complexes.



■ INTRODUCTION

Interaction of macromolecules with solvents is an interesting subject in various fields, such as self-assembly,^{1,2} phase separation,^{3,4} molecular recognition,⁵ complexation,⁶ and crystallization.⁷ The solvent effect is related to the special conformation,⁸ morphology,^{9–11} physical properties,^{9,12} and applied processes^{4,13,14} of macromolecules. Yu et al. presented that the selective solvent can affect the microstructures of polyethylene-*b*-poly(ethylene oxide) assemblies on carbon nanotubes.¹ Wang and Wu investigated gelation of PNIPAM in an ionic liquid, which is caused by formation of new interactions and transformation of interior interaction among polymer chains.¹³ Most recently, Marubayashi et al. confirmed that poly(*L*-lactide) (PLLA) forms crystalline complex (ϵ -form) with solvents of tetrahydrofuran and *N,N*-dimethyl formamide (DMF).⁷ In the PLLA–DMF complex, four PLLA chains and eight guest solvents are proposed to be packed in a unit cell. All of these results demonstrate that interactions between macromolecules and solvents are interesting for both basic and applied aspects. Evaluation of these interactions has great importance for those macromolecules usually used in solutions,

such as polyacrylonitrile (PAN), because their properties definitely depend on the selected solvents.

PAN has become a focus of considerable research for a long time, not only owing to its good mechanical and fiber-forming properties for textiles^{15,16} and membranes,^{17–19} but also as precursors for carbon fibers.^{20–22} A dominant characteristic of PAN is its polar nitrile groups possessing a high dipole moment (3.9 D). The interaction of nitrile groups results in certain physical properties, such as high melting point, serious entanglement of chains, large stiffness, and good solvent resistance.²³ Additionally, the special crystalline structure of PAN is suggested to be a lateral periodicity in the packing of chains without any chain-axis order. However, it is difficult to reach PAN's melted state due to the preoccurrence of decomposition stemming from the cyclization reaction of nitrile groups. This behavior almost makes the melt-processing of PAN impossible. Despite copolymerization with some other monomers, which can reduce the melting point of PAN to

Received: April 30, 2012

Revised: June 17, 2012

Published: June 18, 2012

some extent,^{24–26} the processability of PAN is mainly achieved in solutions with polar organic solvents, such as dimethyl sulfone (DMSO2), dimethyl sulfoxide (DMSO), ethylene carbonate (EC), propene carbonate (PC), DMF, and *N,N*-dimethyl acetamide (DMAc).^{17,27–32} These solvents having polar groups are potentially available for dipole–dipole interaction with the nitrile groups of PAN, which is considered to be a main reason for dissolving PAN. Interestingly, the existence of solvents was proven to influence the physical properties of PAN in solid state.^{33,34} Bashir's group found that DMSO can cocrystallize with PAN, causing a hexagonal to orthorhombic polymorph transition,³³ and γ -butyrolactone or EC can complex with PAN.³⁴ Thermoreversible gelation and plasticization of PAN were also obtained in the concentrated PAN–PC and PAN–DMSO solutions.^{35–37} In addition, different solvents have dissimilar effects on the aggregation of PAN chains and,³⁸ as a consequence, on the morphology and properties of the final products.³⁹ The difference in solvent effects on PAN was assessed by dynamic nuclear magnetic resonance, infrared and Raman spectroscopies.^{40–42} However, it essentially calls for a more detailed interpretation of the origin of these solvent effects. Can we exhaustively study PAN–solvents interactions in terms of both theoretical simulation and experimental analysis, and then link the results with physical behaviors of PAN?

In this work, we discussed the interactions between PAN and various solvents by theoretical calculation based on density functional theories (DFT), and experimental methods of Fourier transform infrared (FTIR) spectra and two-dimensional infrared (2D-IR) correlation analysis. As we know, computational calculation is a simple and fast approach to obtain conformations, binding energies, and vibrational frequencies of interaction molecules and complexes, whereas 2D-IR is a powerful analytical tool for probing subtle and complex changes in 1D IR spectra and is used to elucidate the interaction and structural variation. Our previous work combined DFT calculation and 2D-IR correlation analysis to understand the diffusion process and structural variation of water in PAN containing *N*-vinyl-2-pyrrolidone,⁴ and the recognition mechanism of theophylline-imprinted poly(acrylonitrile-co-acrylic acid).⁵ Herein, we chose DMSO2, DMSO, EC, PC, DMF, and DMAc as the model solvents, while a methyl- and ethyl-ended AN unit (designated as PAN') was used as a PAN model monomer. Calculated results conducted by DFT at B3LYP/6-31+G(d,p) level include the optimized configuration, binding energy, ESP atomic charge, vibrational frequency, and bond length of PAN'–solvent complexes. These results were effectively related to several physical behaviors of PAN reported in earlier studies. Correspondingly, PAN–DMSO, –EC, and –DMF mixtures were measured by concentration-dependent FTIR, and then analyzed by 2D-IR correlation techniques. It shows that these mixtures present different processes of molecular change both for PAN and solvents during concentration. This work may give a foundation to select a solvent for PAN, and provide some insights as to the physical behaviors and properties of PAN or other polar polymers.

EXPERIMENTAL SECTION

Materials. Polyacrylonitrile (PAN, $M_n = 50\,000$ g/mol) was kindly supplied by An Qing Petroleum Chemical Corporation of China. It was crushed finely and dried at 60 °C in an oven before use. Dimethyl sulfone (DMSO2, 99% purity) was purchased from Dakang Chemicals Co., Ltd. of China.

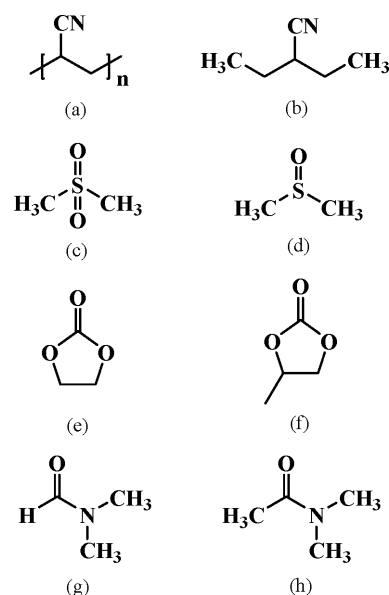


Figure 1. Chemical structures of (a) PAN, (b) methyl- and ethyl-ended AN unit (PAN'), (c) DMSO2, (d) DMSO, (e) EC, (f) PC, (g) DMF, and (h) DMAc.

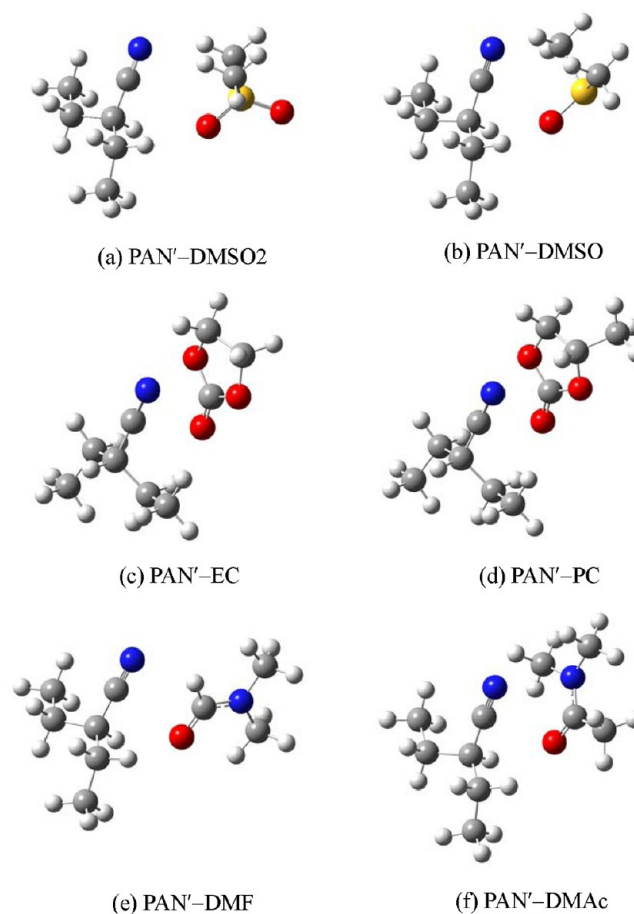


Figure 2. Optimized configurations for (a) PAN'–DMSO2, (b) PAN'–DMSO, (c) PAN'–EC, (d) PAN'–PC, (e) PAN'–DMF, and (f) PAN'–DMAc complexes. They were taken from the energy minimization by DFT calculations. White, gray, blue, yellow, and red balls represent hydrogen, carbon, nitrogen, sulfur, and oxygen atoms, respectively.

Dimethyl sulfoxide (DMSO), *N,N*-dimethyl formamide (DMF), and *N,N*-dimethyl acetamide (DMAc) were commercially

Table 1. Binding Energy (ΔE) Calculated by B3LYP/6-31+G(d,p) Level of Theory

ΔE Hartree (kcal/mol)	PAN'	DMSO2	DMSO	EC	PC	DMF	DMAc
PAN'	−0.00579 (−3.63)	−0.00879 (−5.51)	−0.00856 (−5.37)	−0.00824 (−5.17)	−0.00794 (−4.98)	−0.00632 (−3.97)	−0.00607 (−3.81)
DMSO2	−0.00879 (−5.51)	−0.01317 (−8.27)					
DMSO	−0.00856 (−5.37)		−0.01351 (−8.48)				
EC	−0.00824 (−5.17)			−0.01146 (−7.19)			
PC	−0.00794 (−4.98)				−0.0113 (−7.09)		
DMF	−0.00632 (−3.97)					−0.00688 (−4.32)	
DMAc	−0.00607 (−3.81)						−0.00532 (−3.34)

Table 2. Calculated Interatomic Distance between PAN' and Solvent Molecules

complex	interacting pair	interatomic distance (Å)			included angle ^a (°)
		N→S	N→C	C→O	
PAN'–DMSO2		3.85		3.17	29
PAN'–DMSO		4.25		3.44	35
PAN'–EC			3.45	3.75	15
PAN'–PC			3.50	3.77	12
PAN'–DMF			3.70	3.50	11
PAN'–DMAc			3.68	3.49	10 ^b

^aAngle between the axis of C≡N bond and S=O (or C=O) bond. ^bAn approximate angle because the interaction pair is not in a plane for PAN'–DMAc complex.

obtained from Sinopharm chemical Reagent Co., Ltd. Ethylene carbonate (EC) and propylene carbonate (PC) were brought from Aladdin Chemical Co., Ltd. All solvents are of analytical grade and used as received. Figure 1 presents the chemical structures of all molecules involved in this work.

Computational Methods. To simplify the computational process, a methyl- and ethyl-ended AN unit (PAN') with no chirality was used as a model component representing PAN. The chemical structure of PAN' is as shown in Figure 1(b). The Gaussian 03 program package was applied for all calculations in the present study.⁴³ The geometries of molecular species and PAN'–solvent complexes were optimized using density functional theory (DFT) method based on Becke3LYP (B3LYP) with a 6-31+G(d,p) basis set. Moreover, calculations were performed for the binding energies and the vibrational frequencies of PAN'–solvent complexes. The binding energy was calculated from the equation below:

$$\Delta E = E_{\text{complex}} - (E_{\text{PAN}'} + E_{\text{solvent}})$$

where E_{complex} , $E_{\text{PAN}'}$, and E_{solvent} are energies of PAN'–solvent complex, PAN', and solvent, respectively.

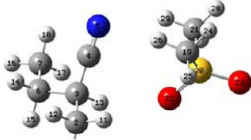
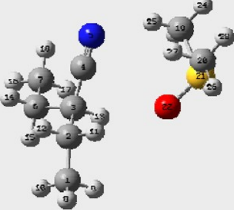

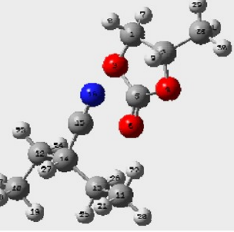
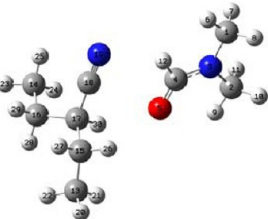
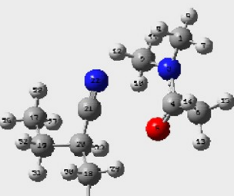
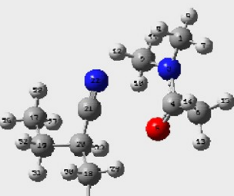
Fourier Transform Infrared Spectroscopy. PAN powder was dissolved in solvents at 60 °C. Several solutions were prepared for PAN–DMSO, PAN–EC, and PAN–DMF mixtures with 5–35 wt.% PAN. Each solution was transformed to sandwich in two pieces of KBr windows, which was used as a transmission cell. FTIR spectra were taken by 32 scans at a nominal resolution of 2 cm^{−1} using a Nicolet Nexus-470 spectrometer. All spectra were baseline-corrected and normalized to the same thickness on the basis of 1453 cm^{−1} assigned to CH bending vibration.

Two-Dimensional Correlation Analysis. 2D-IR correlation analysis using a software program (2Dshige (c) Shigeaki Morita, Kwansei-Gakuin University, Japan, 2004–2005) was conducted for the concentration-dependent FTIR spectra of PAN–DMSO, PAN–EC, and PAN–DMF mixtures, respectively. The normalization of all spectra over concentration was conducted when the integral intensity of peak at 1453 cm^{−1} was chosen as the normalizing factor. The final contour maps were plotted by Sigmaplot 12.0, with different colored regions defined as positive or negative intensities.

RESULTS AND DISCUSSION

Computational Calculations. Since PAN is a polar polymer with a high melting point, it is usually dissolved in a variety of solvents for practical applications. The commonly used solvents are DMSO2, DMSO, EC, PC, DMF, and DMAc, which are highly polar. These solvents dissolve PAN based on interaction, which, in turn, affects the final properties of PAN solutions or even PAN fibers/membranes. Figure 2 shows the optimized configurations of PAN'–solvent complexes by geometry optimization calculations. They all display an antiparallel alignment of interacting pairs between the C≡N group of PAN' and the polar group of solvents (S=O group of DMSO2 or DMSO, C=O group of EC, PC, DMF, or DMAc). Such alignment is a characteristic of dipole–dipole interaction, by which a partially negative portion of a polar molecule is attracted to the partially positive portion of another polar molecule. In view of structure, the antiparallel alignment is good for co-orientation of C≡N, S=O, or C=O groups, which have been reported in PAN–DMSO⁴⁴ and PAN–EC³⁴ mixtures. Dipole–dipole interaction is also found in PAN'–PAN' and solvent–solvent complexes (see Figure S1 of the

Table 3. Calculated ESP Atomic Charges for PAN'–Solvent Complexes, and their Difference Values between Complexes and PAN' Monomer (or Solvent Molecules)^a

complex	configuration	atom	charge in monomer	charge in complex	change ^a
PAN'–DMSO2		C4	0.274	0.295	0.021
		N5	-0.470	-0.465	-0.005
		H13	0.066	0.091	0.025
		S20	1.058	0.885	-0.173
		O22	-0.553	-0.507	0.046
		H26	0.173	0.156	-0.022
PAN'–DMSO		H29	0.178	0.172	-0.006
		C4	0.274	0.343	0.069
		N5	-0.470	-0.536	-0.066
		H13	0.066	0.079	0.013
		S21	0.317	0.283	-0.034
		O22	-0.478	-0.472	0.006
PAN'–EC		H25	0.182	0.197	0.015
		H27	0.166	0.188	0.022
		C16	0.274	0.257	-0.017
		N17	-0.470	-0.456	0.014
		C5	0.912	0.833	-0.079
		O6	-0.565	-0.555	0.010
PAN'–PC		O3	-0.431	-0.406	0.025
		O4	-0.431	-0.375	0.056
		H8	0.050	0.051	0.001
		H9	0.053	0.075	0.022
		C15	0.274	0.296	0.022
		N16	-0.470	-0.488	-0.018
PAN'–DMF		C5	0.907	0.861	-0.046
		O6	-0.553	-0.558	-0.005
		O3	-0.459	-0.423	0.036
		O4	-0.480	-0.457	0.023
		H8	0.044	0.057	0.013
		H9	0.028	0.034	0.006
PAN'–DMAc		C18	0.274	0.337	0.063
		N19	-0.470	-0.519	-0.049
		H30	0.066	0.097	0.031
		C4	0.345	0.265	-0.080
		O5	-0.531	-0.498	0.033
		H12	0.043	0.085	0.042
PAN'–DMAc		C21	0.274	0.386	0.112
		N22	-0.470	-0.530	-0.060
		H33	0.066	0.152	0.086
		C4	0.597	0.678	0.081

^aDifference values of ESP atomic charges between complexes and PAN' monomer (or solvent molecules).

Supporting Information, SI), although only a few C≡N groups in PAN chains can be assumed to be antiparallely aligned with each other due to the low sterical feasibility.⁴⁵ These results suggest that the dissolution of PAN in solvents includes the dissociation of the solvent–solvent complex and the PAN–solvent interaction replacing the inter- or intramolecular interaction of PAN chains.

The molecular structure of solvents is considered as an important factor to understand PAN'–solvent complexes, because the structure affects the accessibility to PAN for interaction. DMSO2 and DMSO are chain molecules having two terminal methyl groups with S=O bond perpendicular to the chain axis, whereas DMF and DMAc are chain molecules with C=O bond but asymmetric structures. Chain molecules

Table 4. Vibrational Frequency (ν , cm^{-1}), Intensity (I , e.u.) and Frequency Change ($\Delta\nu$, cm^{-1})^a Calculated by B3LYP/6-31+G(d,p) Level of Theory

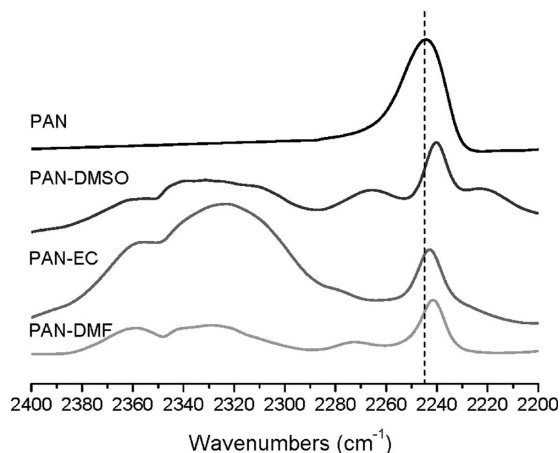
complex	C \equiv N stretching bond			S=O stretching bond			C=O stretching bond		
	ν	I	$\Delta\nu$	ν	I	$\Delta\nu$	ν	I	$\Delta\nu$
PAN'-DMSO2	2332.6	30.2	-9.3	1275.2	261.4	-13.8			
PAN'-DMSO	2330.1	26.3	-11.8	1051.2	124.5	-13.5			
PAN'-EC	2335.5	31.8	-6.4				1867.6	597.7	-30.8
PAN'-PC	2335.4	31.2	-6.5				1865.1	644.4	-29.7
PAN'-DMF	2333.3	22.3	-8.6				1737.1	556.5	-23.5
PAN'-DMAc	2333.1	22.3	-8.8				1706.4	376.0	-18.1

^aDifference value compared with vibrational frequency of PAN' monomer or solvent molecules: 2341.9 cm^{-1} (C \equiv N stretching bond of PAN'), 1289 cm^{-1} (S=O stretching bond of DMSO2), 1064.7 cm^{-1} (S=O stretching bond of DMSO), 1898.4 cm^{-1} (C=O stretching bond of EC), 1894.8 cm^{-1} (C=O stretching bond of PC), 1760.6 cm^{-1} (C=O stretching bond of DMF), and 1724.5 cm^{-1} (C=O stretching bond of DMAc).

Table 5. Calculated Bond Length (l , Å) and Length Change (Δl , pm)^a

complex	C \equiv N bond		S=O bond		C=O bond	
	l (Å)	Δl (pm)	l (Å)	Δl (pm)	l (Å)	Δl (pm)
PAN'-DMSO2	1.162573	0.0395	1.477406	0.3539		
PAN'-DMSO	1.163272	0.1094	1.526777	0.7849		
PAN'-EC	1.162597	0.0419			1.202737	0.6351
PAN'-PC	1.162587	0.0409			1.203200	0.6094
PAN'-DMF	1.162981	0.0803			1.230554	0.6071
PAN'-DMAc	1.162962	0.0784			1.236969	0.5374

^aBond length of PAN' monomer or solvent molecules: 1.162178 Å (C \equiv N bond of PAN'), 1.473867 Å (S=O bond of DMSO2), 1.518928 Å (S=O bond of DMSO), 1.196386 Å (C=O bond of EC), 1.197106 Å (C=O bond of PC), 1.224483 Å (C=O bond of DMF), and 1.231595 Å (C=O bond of DMAc).

**Figure 3.** FTIR spectra in the range of 2400–2200 cm^{-1} . PAN concentration is 5 wt % in the studied mixtures.

are easy to point their outstanding polarized bonds to the nitrile bond attributed to a small volume or good flexibility. As can be seen in Figure 2(a,b), the S=O bond of DMSO2 and DMSO points to the α -hydrogen of PAN' near the nitrile group, while the methyl groups of these solvents push the nitrogen away. In contrast, EC and PC interact with PAN' from the direction opposite to the α -hydrogen of PAN' (Figure 2(c,d)). It may be due to their compact five-member ring structure connected with the C=O bond. Figure 2(e) shows that the PAN'-DMF complex has a similar molecular alignment with those of PAN'-DMSO2 and PAN'-DMSO complexes. As for PAN'-DMAc complex, the C=O bond approaches to the C \equiv N group, keeping the molecular plane of DMAc parallel to the chain axis of PAN' (Figure 2(f)). The discrepancy between the configurations of PAN'-DMF and PAN'-DMAc complexes is because DMAc has a higher steric effect than DMF.⁴⁰

Table 1 lists the calculated binding energy (ΔE) of PAN' interacting with different solvents. ΔE values are in the order of PAN'-DMSO2 < PAN'-DMSO < PAN'-EC < PAN'-PC < PAN'-DMF < PAN'-DMAc, which become more positive from the left to right. It suggests that PAN has a higher inclination to interact with DMSO2 than others. In view of dielectric constants, EC (89.8) and PC (66.1) are more polar than DMSO2 (47.4), DMSO (47.2), DMF (38.3), and DMAc (38.9).⁴⁶ Nevertheless, the six solvents have different molecular structures, as mentioned above. It can be concluded that not only the differences in polarity but also the molecular structures of solvents should be responsible for the differences in ΔE . However, DMSO2, DMSO, EC, and PC interacting with itself are 2–3 kcal/mol lower than those binding with PAN'. For comparison, DMF and DMAc have a similar binding energy no matter whether they interact with themselves or PAN'. It reveals that DMF and DMAc are easier to dissociate with themselves than DMSO2, DMSO, EC, and PC. This result accounts for the facts that DMF and DMAc are the most popular solvents for the applications of PAN at room temperature.

Table 2 shows the interatomic distances in the interacting pairs (N \rightarrow S, N \rightarrow C, and C \rightarrow O). The N \rightarrow S distances are longer than the C \rightarrow O distances in PAN'-DMSO2 and PAN'-DMSO complexes. The N \rightarrow C distances are closed to the C \rightarrow O distances when PAN' interacts with EC, PC, DMF, and DMAc. PAN'-DMSO2 complex has the shortest intermolecular distance (3.17 Å), indicating the most compact structure. This structure of the PAN'-DMSO2 complex may be ascribed to its lowest binding energy of interaction (Table 1). Besides, PAN'-DMSO2 and PAN'-DMSO complexes have larger included angles than others owing to the methyl groups of DMSO2 and DMSO perpendicular to the chain axis.

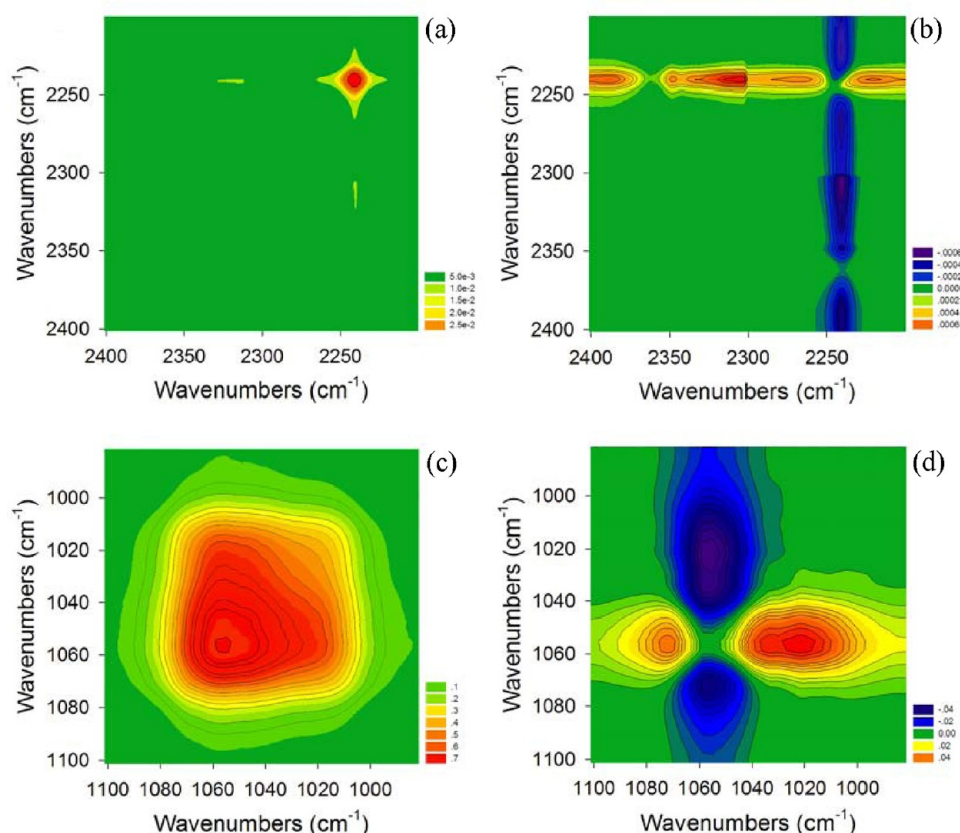


Figure 4. (a,c) Synchronous and (b,d) asynchronous 2D correlation contour maps of concentration-dependent FTIR spectra for PAN–DMSO mixture in the spectral ranges of (a,b) 2400–2200 cm^{-1} and (c,d) 1100–980 cm^{-1} .

Apart from the interatomic distances, ESP atomic charges of PAN'–solvent complex are collected in Table 3. After complexation, the carbon atom and the nitrogen atom in the $\text{C}\equiv\text{N}$ bond respectively become more positive and more negative, except for in the PAN'–EC complex. It indicates that the $\text{C}\equiv\text{N}$ bond becomes more polarized and thus enhances the chemical activity of the $\text{C}\equiv\text{N}$ bond. It can explain why a small amount of solvents is favorable for the cyclization of PAN at a relative low temperature. Additionally, the change of charges is also found in neighboring atoms, such as the α -hydrogen of PAN' near the nitrile group, the hydrogen in the methyl groups of DMSO2 and DMSO, the oxygen in the carbonate ring, and the α -hydrogen of the DMF. The neighboring atoms may participate in the interaction and stabilize the complexes. Saum et al. reported that intermolecular hydrogen bonding between $\text{C}\equiv\text{N}$ and $\text{C}-\text{H}$ is important for the fiber-forming capacity of PAN.⁴⁷ Nevertheless, the energy of a hydrogen bond of the type $\text{N}\cdots\text{H}-\text{C}$ is considered to be smaller than that of dipole–dipole interaction.⁴⁵

These calculated results can be related to the solvent effects on acrylonitrile polymerization. EC was found to be better than DMSO and DMF for reversible addition-fragmentation chain transfer (RAFT) polymerization of acrylonitrile in the presence of 2-cyanoprop-2-yl dithiobenzoate.³⁸ Calculations for model compounds carried out in the present study show that the electron cloud of $\text{C}\equiv\text{N}$ bond becomes even after interacting with EC. This change would enhance the stability of free radicals and prevent the termination of RAFT polymerization. Thus, when using EC as solvent, the obtained PAN has a much

higher molecular weight and lower polydispersity than those polymerized in DMSO or DMF.

The shift in vibrational frequency is always used to assess the interactions. Herein, the vibrational frequency for PAN'–solvent complexes was calculated (Table 4). Red shift of vibrational frequencies is observed for $\text{C}\equiv\text{N}$, $\text{S}=\text{O}$, and $\text{C}=\text{O}$ stretching bonds either in PAN'–PAN', solvent–solvent, or in PAN'–solvent complexes. As for $\text{C}\equiv\text{N}$ stretching bond, the degree of red shift is in the order of $\text{DMSO} > \text{DMSO2} > \text{DMAc} > \text{DMF} > \text{PC} > \text{EC}$. This is not consistent with the bonding energy of complexes (Table 1), suggesting the nonequivalence between the interaction strength and the red shift of vibrational frequency. According to quantum mechanics, the frequency of the stretching vibration is directly proportional to the square root of the mechanical constant, which is correlated to the change of electric dipole moment. The dipole moment changes as the bond becomes shorter or longer. As listed in Table 5, the length of the $\text{C}\equiv\text{N}$ bond in the PAN'–DMSO complex shows the most significant change, corresponding to the largest shift of the vibrational frequency. However, in the PAN'–DMSO2 complex, the small change of bond length may not be commensurate with the high shift for the vibrational frequency of $\text{C}\equiv\text{N}$ stretching bond.

FT-IR Spectra and 2D-IR Correlation Analysis. FTIR spectroscopy is a powerful tool to probe interactions between polymers and small molecules. A significant characteristic is the shift of vibrational frequency stemming from the change of the chemical surrounding. Litovchenko et al. compared the vibrational frequency of $\text{C}\equiv\text{N}$ groups in solid bulk and in organic solvents (DMF, DMAc, and DMSO), which shifted from 2247 to 2243 cm^{-1} .⁴² We compared the FTIR spectra of

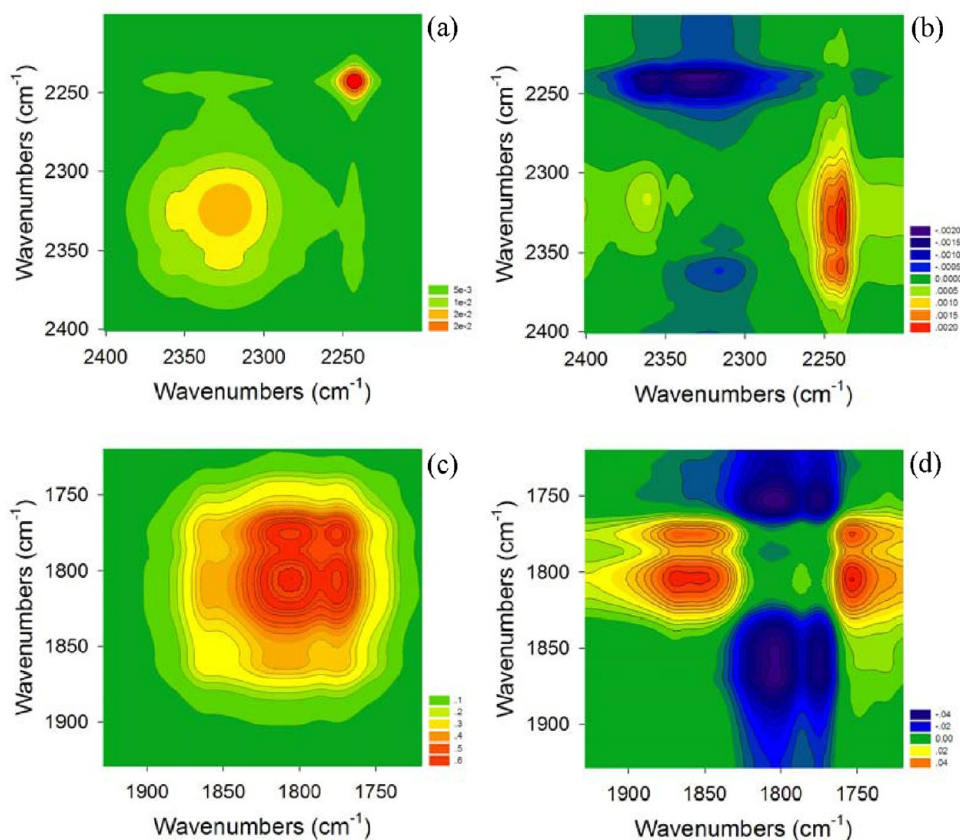


Figure 5. (a,c) Synchronous and (b,d) asynchronous 2D correlation contour maps of concentration-dependent FTIR spectra for PAN–EC mixture in the spectral ranges of (a,b) 2400–2200 cm^{-1} and (c,d) 1928–1720 cm^{-1} .

PAN–DMSO, PAN–EC, and PAN–DMF mixtures. As shown in Figure 3, a peak at 2245 cm^{-1} is assigned for $\text{C}\equiv\text{N}$ stretching of PAN, whereas it shifts to 2240, 2242, and 2241 cm^{-1} as PAN is dissolved in DMSO, EC, and DMF, respectively. This experimental result is consistent with calculation by DFT, in which $\text{C}\equiv\text{N}$ groups in PAN–EC system show the smallest frequency change (Table 4). Moreover, a wide absorption band comes out around 2320 cm^{-1} for the mixtures, which is different from those of pure DMSO, EC, DMF, or PAN (see Figure S2 of the SI). It is due to the interaction between PAN and solvent molecules according to literature.³² Besides, the vibrational frequency for $\text{C}\equiv\text{N}$ stretching band almost keeps constant as PAN content increases (see Figure S3 of the SI). On the other hand, changes for $\text{S}=\text{O}$ and $\text{C}=\text{O}$ stretching bands are the most considerable ones although the red-shifts are weak (see Figure S4 of the SI). In contrast, it is identical for the frequency range of $\text{C}-\text{H}$ stretching vibrations (3150–2800 cm^{-1}) despite the calculated atomic charges vary to a certain degree (Table 3). It suggests that the direct interactions are not via CH_2 and CH_3 groups but via dipole–dipole interaction between $\text{C}\equiv\text{N}$ groups and $\text{S}=\text{O}$ or $\text{C}=\text{O}$ groups. Particularly, as for the PAN–EC mixture, both vibration bands at 1070 and 1157 cm^{-1} shift to high frequencies, which are assigned to the ring breathing and the skeletal stretching of EC, respectively (see Figure S5 of the SI). We can conclude that the ring should be an important part in PAN–EC interaction.

2D-IR correlation analysis was further applied to capture subtle information that is not obvious in 1D spectra. Figure 4(a,b) shows the synchronous and asynchronous correlation spectra of the PAN–DMSO mixture in the region of 2400–2200 cm^{-1} .

In the synchronous map, an autopeak appears at 2241 cm^{-1} , corresponding to the absorption band in 1D spectra (Figure 3). This autopeak has an elongated shape extended to 2300 cm^{-1} and 2221 cm^{-1} , which suggests that two cross-peaks form by 2241/2265 cm^{-1} and 2241/2221 cm^{-1} bands. Another elongated positive cross-peak is revealed at 2327/2241 cm^{-1} . The positive sign of the cross-peak indicates that both bands become strong as the PAN content increases. In the asynchronous map, there are three positive bands (2265/2241, 2305/2241, and 2389/2241 cm^{-1}), and one negative band (2241/2220 cm^{-1}). The 2241 and 2265 cm^{-1} bands represent $\text{C}\equiv\text{N}$ groups in PAN bulk, but they are assigned to different intermolecular interactions.⁴⁸ Bands at 2305 and 2220 cm^{-1} are related to PAN–DMSO interaction. According to Noda,⁴⁹ if $\Phi(\nu_1, \nu_2) > 0$ and $\Psi(\nu_1, \nu_2)$ is positive, then the ν_1 band will change prior to the ν_2 band; if $\Psi(\nu_1, \nu_2)$ is negative, then ν_1 will vary behind ν_2 . If $\Phi(\nu_1, \nu_2) < 0$, then the rule is reversed. Therefore, as the PAN content increases, PAN–DMSO complexes change earlier than the PAN bulk.

Figure 4(c,d) shows the calculated synchronous and asynchronous correlation spectra in the region of 1100–980 cm^{-1} . It is clear that an autopeak is located at 1058 cm^{-1} in the synchronous map. Accordingly, one positive cross-peak (1072/1058 cm^{-1}) and one negative cross-peak (1058/1020 cm^{-1}) are observed in the asynchronous map, indicating that the broad $\text{S}=\text{O}$ stretching band is split into three separate bands at 1072, 1058, and 1020 cm^{-1} . The bands of 1072 and 1020 cm^{-1} are assigned to the $\text{S}=\text{O}$ stretching band of free DMSO molecule and DMSO dimer, respectively.⁵⁰ The 1058 cm^{-1} band corresponds to the dipole–dipole interaction between DMSO and PAN, which is in line with the calculated vibrational

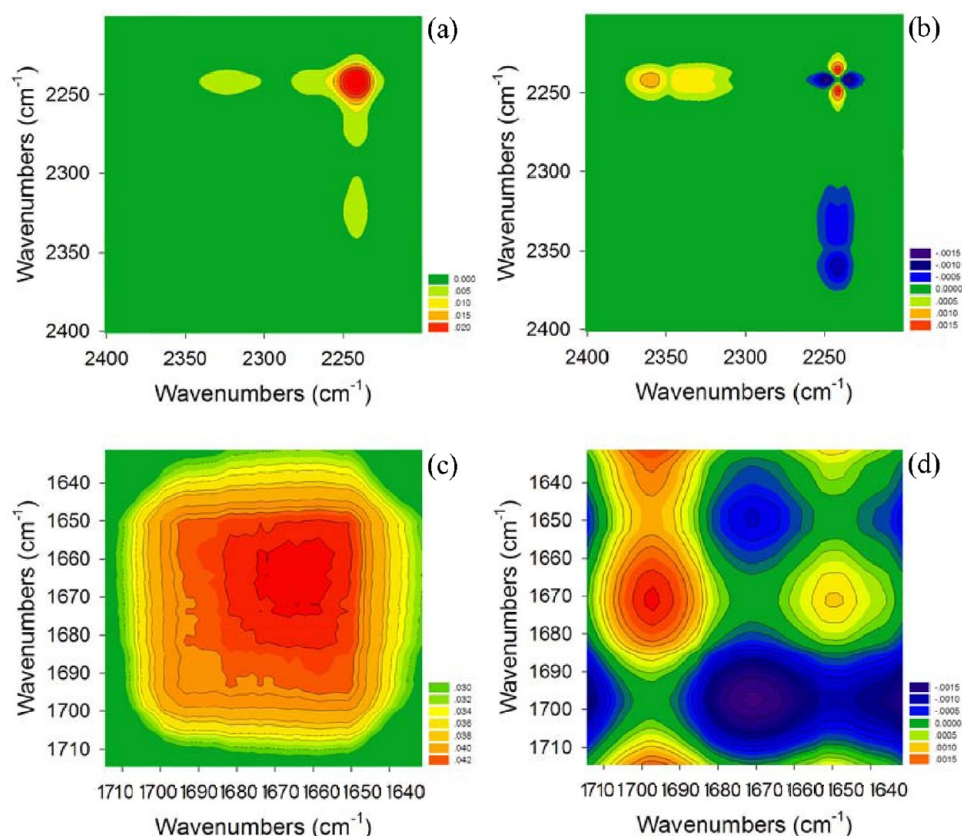


Figure 6. (a,c) Synchronous and (b,d) asynchronous 2D correlation contour maps of concentration-dependent FTIR spectra for PAN–DMF mixture in the spectral ranges of (a,b) 2400–2200 cm^{-1} and (c,d) 1713–1573 cm^{-1} .

frequency of 1051 cm^{-1} . The free DMSO molecule (1072 cm^{-1}) and the DMSO dimer (1020 cm^{-1}) vary prior to PAN–DMSO complexes (1058 cm^{-1}).

A different pattern presents itself in the synchronous and asynchronous correlation spectra of the PAN–EC mixture. Figure 5a shows that two autopeaks are located at 2243 and 2324 cm^{-1} and an elongated positive cross-peak is revealed at 2335/2243 cm^{-1} in the synchronous map, whereas two positive cross-peaks (2239/2227 and 2362/2316 cm^{-1}) and two negative cross-peaks (2359/2237 and 2330/2239 cm^{-1}) are in the asynchronous one (Figure 5b). The bands of 2243, 2239, and 2237 cm^{-1} are assigned to the $\text{C}\equiv\text{N}$ stretching band in PAN bulk, whereas the 2227 cm^{-1} band is assigned to the $\text{C}\equiv\text{N}$ stretching band in PAN–EC complexes. According to the literature,³² 2330 cm^{-1} indicates the dipole–dipole interaction between PAN and EC. As for the $\text{C}=\text{O}$ groups (Figure 5(c,d)), two autopeaks are observed at 1774 and 1805 cm^{-1} , and a positive cross-peak is revealed at 1805/1774 cm^{-1} in the synchronous map. Three negative cross-peaks (1805/1753, 1774/1753, and 1807/1786 cm^{-1}) and two positive cross-peaks (1886/1776 and 1886/1801 cm^{-1}) are observed in the asynchronous map. The bands at 1807, 1805, 1774, and 1776 cm^{-1} are due to the $\text{C}=\text{O}$ stretching of EC molecule, while 1786 and 1753 cm^{-1} are due to the $\text{C}=\text{O}$ stretching of EC that participates in the dipole–dipole interaction with PAN. Accordingly, EC molecules vary slower than PAN–EC complexes, and both of them change after PAN bulk. Besides, the $\text{C}=\text{O}$ stretching band of EC varies prior to the ring breathing and skeletal stretching as PAN content increasing (see Figure S6 of the SI).

The PAN–DMF mixture shows a similar result with the PAN–EC one. As shown in Figure 6(a,b), the autopeak at 2241 cm^{-1} in the synchronous plot splits into one positive cross-peak (2241/2235 cm^{-1}) and one negative cross-peak (2248/2241 cm^{-1}) presenting in the asynchronous map. Correspondingly, in the range of 1713–1630 cm^{-1} , an autopeak is revealed at 1666 cm^{-1} in the synchronous map. In the asynchronous plot, there are a positive (1697/1672 cm^{-1}) and a negative cross-peak (1672/1648 cm^{-1}). According to the Noda rule, it can be concluded that PAN bulk (2241 and 2248 cm^{-1}) varies prior to PAN–DMF complexes (2235, 1697, and 1648 cm^{-1}) and change earlier than DMF molecules (1666 and 1672 cm^{-1}).

CONCLUSIONS

Interactions have been theoretically calculated based on DFT and experimentally investigated by concentration-dependent FTIR spectra and 2D-IR correlation analysis for mixtures of PAN and various solvents including DMSO₂, DMSO, EC, PC, DMF, and DMAc. (1) PAN model monomer (PAN') interacts with the solvents through dipole–dipole interaction, by which an antiparallel alignment is displayed between the $\text{C}\equiv\text{N}$ group of PAN' and the polar group of solvent molecule ($\text{S}=\text{O}$ or $\text{C}=\text{O}$ group). (2) Calculated binding energies (ΔE) are in the order of $\text{PAN}'\text{-DMSO}_2 < \text{-DMSO} < \text{-EC} < \text{-PC} < \text{-DMF} < \text{-DMAc}$, which results from the polarity and molecular structure of solvents. However, this order of ΔE is different from that of the red shift of calculated vibrational frequency for $\text{C}\equiv\text{N}$, $\text{S}=\text{O}$, and $\text{C}=\text{O}$ stretching bands, suggesting the nonequivalence between the interaction strength and the red shift of vibrational frequency. (3) Calculated ESP atomic

charges reveal that the carbon atom and the nitrogen atom in the C≡N bond are respectively less positive and less negative only in the PAN'-EC complex, indicating that the electron cloud of the C≡N bond becomes even. These results provide an explanation for the solvent effects on reversible addition-fragmentation chain transfer polymerization of acrylonitrile reported previously. (4) FTIR spectra show the red shifts of vibrational frequency for C≡N stretching band in PAN-DMSO, -EC, and -DMF mixtures, indicating the PAN-solvent interactions. Moreover, the 2D-IR correlation analysis in the $\nu(\text{C}\equiv\text{N})$, $\nu(\text{S}=\text{O})$, and $\nu(\text{C}=\text{O})$ regions demonstrates that as the PAN content increases, DMSO molecules vary prior to PAN-DMSO complexes, both of which change earlier than PAN bulk. However, the PAN-EC and PAN-DMF mixtures present the molecular change in the order of PAN bulk > PAN-solvent complex > solvent molecules. All of these theoretical and experimental results may be a foundation to support and understand a number of physical phenomena of PAN or other polar polymers.

■ ASSOCIATED CONTENT

● Supporting Information

Optimized configurations and FTIR spectra. This material is available free of charge via the Internet at <http://pubs.acs.org>.

■ AUTHOR INFORMATION

Corresponding Author

*Fax: + 86 571 8795 1773; E-mail: xuzk@zju.edu.cn.

Author Contributions

[†]Both authors contributed equally to the present work.

Notes

The authors declare no competing financial interest.

■ ACKNOWLEDGMENTS

This work was financially supported by the National Natural Science Foundation of China (Grant No. 21174124). The authors thank Dr. Jun Ling at Zhejiang University for helping the computational calculations.

■ REFERENCES

- (1) Yu, N.; Zheng, X.; Xu, Q.; He, L. *Macromolecules* **2011**, *44*, 3958–3965.
- (2) Huang, W.-H.; Chen, P.-Y.; Tung, S.-H. *Macromolecules* **2012**, *45*, 1562–1569.
- (3) Nakamura, I.; Shi, A. C. *J. Phys. Chem. B* **2011**, *115*, 2783–2790.
- (4) Wan, L.-S.; Huang, X.-J.; Xu, Z.-K. *J. Phys. Chem. B* **2007**, *111*, 922–928.
- (5) Che, A.-F.; Wan, L.-S.; Ling, J.; Liu, Z.-M.; Xu, Z.-K. *J. Phys. Chem. B* **2009**, *113*, 7053–7058.
- (6) Tallury, S. S.; Smyth, M. B.; Cakmak, E.; Pasquinelli, M. A. *J. Phys. Chem. B* **2012**, *116*, 2023–2030.
- (7) Marubayashi, H.; Asai, S.; Sumita, M. *Macromolecules* **2012**, *45*, 1384–1397.
- (8) Nomura, A.; Okayasu, K.; Ohno, K.; Fukuda, T.; Tsujii, Y. *Macromolecules* **2011**, *44*, 5013–5019.
- (9) Wu, S.; Zhang, Q.; Bubeck, C. *Macromolecules* **2010**, *43*, 6142–6151.
- (10) He, L.; Zheng, X.; Xu, Q. *J. Phys. Chem. B* **2010**, *114*, 5257–5262.
- (11) Hartikainen, J.; Lehtonen, O.; Harmia, T.; Lindner, M.; Valkama, S.; Ruokolainen, J.; Friedrich, K. *Chem. Mater.* **2004**, *16*, 3032–3039.
- (12) Shang, B. Z.; Wang, Z.; Larson, R. G. *J. Phys. Chem. B* **2009**, *113*, 15170–15180.
- (13) Wang, Z.; Wu, P. *J. Phys. Chem. B* **2011**, *115*, 10604–10614.
- (14) Tang, B.; Wu, P. *Vib. Spectrosc.* **2009**, *51*, 65–71.
- (15) Hussain, D.; Loyal, F.; Greiner, A.; Wendorff, J. H. *Polymer* **2010**, *51*, 3989–3997.
- (16) Zander, N. E.; Strawhecker, K. E.; Orlicki, J. A.; Rawlett, A. M.; Beebe, T. P. *J. Phys. Chem. B* **2011**, *115*, 12441–12447.
- (17) Wan, L.-S.; Xu, Z.-K.; Huang, X.-J.; Che, A.-F.; Wang, Z.-G. *J. Membr. Sci.* **2006**, *277*, 157–164.
- (18) Tsai, H.-A.; Ye, Y.-L.; Lee, K.-R.; Huang, S.-H.; Suen, M.-C.; Lai, J.-Y. *J. Membr. Sci.* **2011**, *368*, 254–263.
- (19) Wang, Z. G.; Wan, L. S.; Xu, Z. K. *J. Membr. Sci.* **2007**, *304*, 8–23.
- (20) Osbeck, S.; Bradley, R. H.; Liu, C.; Idriss, H.; Ward, S. *Carbon* **2011**, *49*, 4322–4330.
- (21) Shen, W.; Zhang, S.; He, Y.; Li, J.; Fan, W. *J. Mater. Chem.* **2011**, *21*, 14036–14040.
- (22) Rahaman, M. S. A.; Ismail, A. F.; Mustafa, A. *Polym. Degrad. Stab.* **2007**, *92*, 1421–1432.
- (23) Lachat, V.; Varshney, V.; Dhinojwala, A.; Yeganeh, M. S. *Macromolecules* **2009**, *42*, 7103–7107.
- (24) Deng, W.; Lobovsky, A.; Iacono, S. T.; Wu, T.; Tomar, N.; Budy, S. M.; Long, T.; Hoffman, W. P.; Smith, D. W., Jr. *Polymer* **2011**, *52*, 622–628.
- (25) Naskar, A. K.; Walker, R. A.; Proulx, S.; Edie, D. D.; Ogale, A. A. *Carbon* **2005**, *43*, 1065–1072.
- (26) Godshall, D.; Rangarajan, P.; Baird, D. G.; Wilkes, G. L.; Bhanu, V. A.; McGrath, J. E. *Polymer* **2003**, *44*, 4221–4228.
- (27) Wu, Q. Y.; Wan, L. S.; Xu, Z. K. *J. Membr. Sci.* **2012**, *409*–410, 355–364.
- (28) Che, A.-F.; Huang, X.-J.; Xu, Z.-K. *J. Membr. Sci.* **2011**, *366*, 272–277.
- (29) Wang, Z. G.; Xu, Z. K.; Wan, L. S. *J. Membr. Sci.* **2006**, *278*, 447–456.
- (30) Yoon, K.; Hsiao, B. S.; Chu, B. *J. Membr. Sci.* **2009**, *338*, 145–152.
- (31) Chu, P. P.; He, Z. P. *Polymer* **2001**, *42*, 4743–4749.
- (32) Ostrovskii, D.; Brodin, A.; Torell, L. M.; Appetecchi, G. B.; Scrosati, B. *J. Chem. Phys.* **1998**, *109*, 7618–7624.
- (33) Bashir, Z. *J. Polym. Sci., Part B* **1994**, *32*, 1115–1128.
- (34) Bashir, Z.; Church, S. P.; Price, D. M. *Acta Polym.* **1993**, *44*, 211–218.
- (35) Bashir, Z. *Polymer* **1992**, *33*, 4304–4313.
- (36) Tan, L. J.; Pan, D.; Pan, N. *Polymer* **2008**, *49*, 5676–5682.
- (37) Tan, L.; Liu, S.; Pan, D. *J. Phys. Chem. B* **2009**, *113*, 603–609.
- (38) Liu, X.-H.; Li, Y.-G.; Lin, Y.; Li, Y.-S. *J. Polym. Sci., Part A* **2007**, *45*, 1272–1281.
- (39) Mahmod, D. S. A.; Ismail, A. F.; Mustafa, A.; Ng, B. C.; Abdullah, M. S. *J. Appl. Polym. Sci.* **2011**, *121*, 2467–2472.
- (40) Minagawa, M.; Takasu, T.; Morita, T.; Shirai, H.; Fujikura, Y.; Kameda, Y. *Polymer* **1996**, *37*, 463–467.
- (41) Minagawa, M.; Shirai, H.; Morita, T.; Fujikura, Y.; Kameda, Y. *Polymer* **1996**, *37*, 2353–2358.
- (42) Litovchenko, G. D.; Girshgorn, V. M. *J. Appl. Spectrosc.* **1980**, *32*, 170–172.
- (43) Frisch, M. J.; Trucks, G. W.; Schlegel, H. B.; Scuseria, G. E.; Robb, M. A.; Cheeseman, J. R.; Zakrzewski, V. G.; Montgomery, J. A.; Stratmann, R. E.; Burant, J. C.; Dapprich, S.; Millam, J. M.; Daniels, A. D.; Kudin, K. N.; Strain, M. C.; Farkas, O.; Tomasi, J.; Barone, V.; Cossi, M.; Cammi, R.; Mennucci, B.; Pomelli, C.; Adamo, C.; Clifford, S.; Ochterski, J.; Petersson, G. A.; Ayala, P. Y.; Cui, Q.; Morokuma, K.; Malick, D. K.; Rabuck, A. D.; Raghavachari, K.; Foresman, J. B.; Cioslowski, J.; Ortiz, J. V.; Stefanov, B. B.; Liu, G.; Liashenko, A.; Piskorz, P.; Komaromi, I.; Gomperts, R.; Martin, R. L.; Fox, D. J.; Keith, T.; Al-Laham, M. A.; Peng, C. Y.; Nanayakkara, A.; Gonzalez, C.; Challacombe, M.; Gill, P. M. W.; Johnson, B. G.; Chen, W.; Wong, M. W.; Andres, J. L.; Head-Gordon, M.; Replogle, E. S.; Pople, J. A. *Gaussian 03, revision C.02*; Gaussian Inc.: Wallingford, CT: 2004.
- (44) Bashir, Z.; Tipping, A. R.; Church, S. P. *Polym. Int.* **1994**, *33*, 9–17.

- (45) Henrici-Olivé, G.; Olivé, S. *Adv. Polym. Sci.* **1979**, *32*, 123.
- (46) Lide, D. R., Ed. *CRC Handbook of Chemistry and Physics*, 90th ed.; CRC Press: Boca Raton, FL, 2010.
- (47) Saum, A. M. *J. Polym. Sci.* **1960**, *42*, 57–66.
- (48) Yamada, T.; Graham, J. L.; Minus, D. K. *Energy Fuels* **2009**, *23*, 443–450.
- (49) Noda, I. *J. Am. Chem. Soc.* **1989**, *111*, 8116–8118.
- (50) Fawcett, W. R.; Kloss, A. A. *J. Phys. Chem.* **1996**, *100*, 2019–2024.